

See discussions, stats, and author profiles for this publication at: <https://www.researchgate.net/publication/234041820>

# Experimental and Theoretical Insights into the Involvement of Radicals in Triclosan Phototransformation

ARTICLE *in* ENVIRONMENTAL SCIENCE & TECHNOLOGY · JANUARY 2013

Impact Factor: 5.33 · DOI: 10.1021/es3041797 · Source: PubMed

---

CITATIONS

16

---

READS

77

## 4 AUTHORS, INCLUDING:



**Sarah Kliegman**

Reed College

5 PUBLICATIONS 68 CITATIONS

SEE PROFILE



**William A Arnold**

University of Minnesota Twin Cities

119 PUBLICATIONS 3,924 CITATIONS

SEE PROFILE



**Kristopher McNeill**

ETH Zurich

126 PUBLICATIONS 3,439 CITATIONS

SEE PROFILE

# Experimental and Theoretical Insights into the Involvement of Radicals in Triclosan Phototransformation

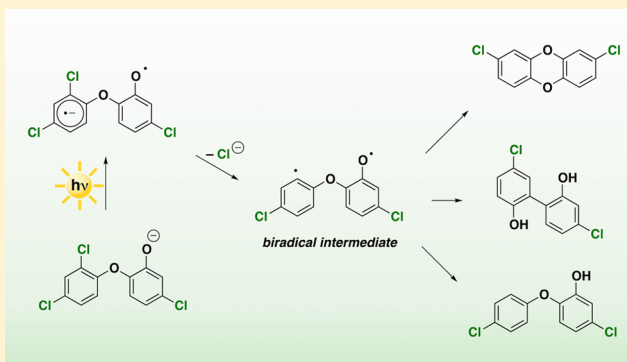
Sarah Kliegman,<sup>†</sup> Soren N. Eustis,<sup>†,‡</sup> William A. Arnold,<sup>‡</sup> and Kristopher McNeill<sup>\*,†</sup>

<sup>†</sup>Institute for Biogeochemistry and Pollutant Dynamics, ETH Zurich, 8092 Zurich, Switzerland

<sup>‡</sup>Department of Civil Engineering, University of Minnesota, 500 Pillsbury Drive SE, Minneapolis, Minnesota 55455, United States

## S Supporting Information

**ABSTRACT:** The phototransformation of triclosan has been a matter of longstanding interest due to both its prevalence in the environment and the discovery of 2,8-dichlorodibenzodioxin as a photoproduct. In this study, photolysis of triclosan resulted in several primary photoproducts including the following: 2,8-dichlorodibenzodioxin (4%), 4,5'-dichloro-[1,1'-biphenyl]-2,2'-diol (10%), 5-chloro-2-(4-chlorophenoxy)phenol (0.5%), and 2,4-dichlorophenol (7%). Trapping studies using *d*<sub>8</sub>-isopropanol showed deuterium incorporation in 5-chloro-2-(4-chlorophenoxy)phenol, providing strong evidence for the involvement of organic radicals in this reaction. Density functional calculations of the excited states of triclosan support the involvement of a radical intermediate in the mechanisms responsible for the dioxin, biphenyl, and phenoxyphenol photoproducts. The pathways for C–Cl bond cleavage and cyclization reactions are discussed.



## INTRODUCTION

Triclosan (5-chloro-2-(2,4-dichlorophenoxy)phenol), a widely used additive in consumer products due to its antibacterial and antifungal properties, has become a frequently detected contaminant in wastewater effluents,<sup>1,2</sup> surface waters,<sup>2,3</sup> and sediments.<sup>2,4,5</sup> Triclosan is known to undergo a variety of partitioning and degradation processes in the aquatic environment, including direct (unsensitized) photochemical degradation leading to a variety of photoproducts.<sup>2,6,7</sup> Concern about the potential ecotoxicological effects of triclosan and its degradation products in the environment encouraged efforts to identify these products and quantify their toxicity.<sup>8</sup>

Direct photolysis has been found to be an important loss process for triclosan in the environment.<sup>2,6,7</sup> Due in part to higher light absorption in the near-UV region of the solar spectrum, triclosan ( $pK_a$  8.1) is more photochemically labile in the phenolate form<sup>7,9,10</sup> and degrades readily yielding a range of products (Figure 1). There are four major photoproducts that have been identified previously: 2,8-dichlorodibenzodioxin (2,8-DCDD) resulting from cyclization (Figure 1, process I);<sup>9–14</sup> 4,5'-dichloro-[1,1'-biphenyl]-2,2'-diol ((OH)<sub>2</sub>PCB-13) involving a skeletal rearrangement from a diphenyl ether to a hydroxylbiphenyl core structure (II);<sup>10</sup> lower chlorinated triclosan derivatives resulting from hydrodehalogenation reactions or replacement of a chlorine substituent by a hydrogen atom, (III);<sup>15</sup> and, dichlorophenol resulting from ether cleavage (IV).<sup>15</sup> In addition, polymerization (V) occurs at high triclosan concentrations (100  $\mu$ M).<sup>9,16</sup> In the aquatic environment, where triclosan concentrations are in the

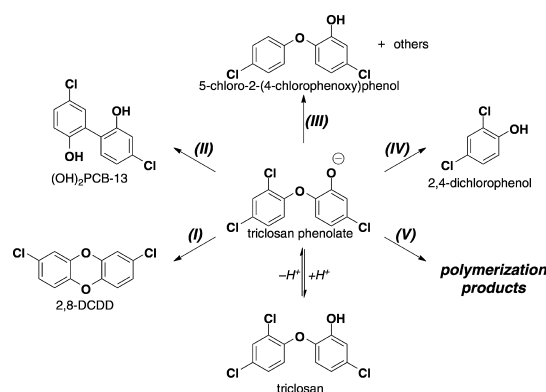


**Figure 1.** Products observed from photochemical degradation of triclosan under basic conditions.

subnanomolar range,<sup>2</sup> processes I–IV, which involve only a single triclosan molecule, are expected to dominate.

The mechanisms of the transformation processes are not yet fully understood. For example, although photocyclization of halogenated phenoxyphenols leading to dioxins has been observed with triclosan,<sup>9–14</sup> more highly chlorinated phenoxy-

**Special Issue:** Rene Schwarzenbach Tribute

**Received:** October 12, 2012

**Revised:** December 27, 2012

**Accepted:** January 2, 2013

**Published:** January 2, 2013

yphenols (4–9 chlorine atoms),<sup>17–21</sup> and brominated phenoxyphenols,<sup>22,23</sup> the nature of the excited state involved and the identity of the important chemical intermediates are not yet known. A better understanding of the structures and mechanisms that lead to potentially toxic products may be useful for modeling of environmental fate and smart chemical design.

It is noteworthy that 2,8-DCDD, (OH)<sub>2</sub>PCB-13, and the lower chlorinated phenoxyphenol products are dechlorinated with respect to the parent compound, necessitating a C–Cl bond cleavage step in the mechanism. There are at least three possibilities for this reaction (Figure 2). The bond cleavage

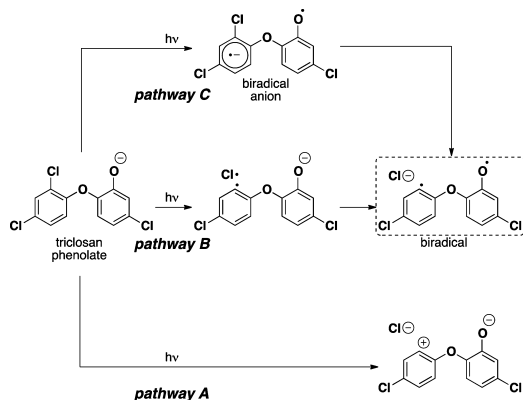


**Figure 2.** Possible mechanisms for photochemically mediated C–Cl bond cleavage in triclosan. Pathway A represents heterolytic carbon chlorine bond cleavage. In pathway B, the carbon chlorine bond is cleaved homolytically and intermolecular electron transfer can give rise to a biradical. In pathway C, intramolecular electron transfer following excitation yields a biradical anion that undergoes cleavage to form a biradical.

could be heterolytic giving a phenyl carbocation and chloride (pathway A). Alternatively, homolytic C–Cl cleavage could occur, giving a chlorine atom and a phenyl radical (pathway B). Finally, a reductive dechlorination pathway (C) could be operative, involving first an intramolecular electron transfer from the phenoxide ring to the dichlorophenoxy ring giving a biradical anion, followed by loss of chloride anion to give a biradical.<sup>21,24</sup>

The motivation for the present work was an interest in the relative importance of the various transformation pathways and the mechanisms and intermediates involved in these reactions. In this study, product formation was quantified, and the involvement of organic radicals was confirmed with trapping studies. In addition, the energetics of the ground and first excited singlet states of triclosan and electron density distributions were calculated. Based on the results of this work, we favor the involvement of a biradical intermediate formed via pathway C. This biradical is further believed to be the key intermediate that leads to the formation of 2,8-DCDD, (OH)<sub>2</sub>PCB-13, and a dichloro analogue of triclosan: 5-chloro-2-(4-chlorophenoxy)phenol.

## EXPERIMENTAL SECTION

**Chemicals.** Triclosan (Irgasan) 2,4-dichlorophenol, *d*<sub>8</sub>-isopropanol (99% deuterium), sodium chloride (NaCl), sodium bromide (NaBr), potassium thiocyanate (KSCN), sodium carbonate (Na<sub>2</sub>CO<sub>3</sub>), sodium bicarbonate (NaHCO<sub>3</sub>), and isopropanol were purchased from Aldrich,

and potassium peroxydisulfate (K<sub>2</sub>S<sub>2</sub>O<sub>8</sub>) was purchased from Acros. Formic acid (98–100%), methanol, and acetonitrile were purchased from Merck. Standards of 2,2-biphenol and 2-phenoxyphenol were purchased from TCI; 2,8-dichlorodibenzodioxin was purchased from AccuStandard. Solvents were all HPLC grade, and all purchased chemicals were used as received. Standards of hydroxylated chlorinated biphenyls<sup>25</sup> and chlorinated phenoxyphenols were prepared<sup>17,26,27</sup> using previously described methods.

**General.** Photolysis studies were conducted in 20 mL Pyrex tubes with screw caps. The photolysis solution consisted of triclosan (50 μM) dissolved in carbonate buffer (0.01 M, pH 10.6; NaHCO<sub>3</sub> (121.3 mg), Na<sub>2</sub>CO<sub>3</sub> (293.1 mg), water (1 L)) containing 10% methanol. The solutions were photolyzed in a Rayonet photoreactor fitted with a merry-go-round apparatus and two 300 nm wavelength bulbs. Time points were taken over the course of approximately ten minutes. The photolysate was analyzed without further processing using HPLC with diode array detection and nUPLC coupled to a mass spectrometer. HPLC analyses were completed using a Dionex P680 Pump, PDA-100 Detector, ASI-100 Automatic sample injector HPLC system fitted with a Discovery RP-Amide column (15 cm × 4.6 mm × 5 μm). An isocratic method using 60:40 acetonitrile:pH 3 formate buffer (5 mM formic acid adjusted with sodium hydroxide to pH 3, 10% acetonitrile) at a flow rate of 1 mL/min was used. Products were identified using authentic standards by matching their retention time and absorbance spectra. nUPLC-MS analyses were performed using a Waters nanoAcuity nUPLC coupled to a Thermo Exactive Mass spectrometer with an electrospray ionization (ESI) source and an Orbitrap mass analyzer. The nUPLC was fitted with a Phenomenex Synergi 4u Max-RP 80 Å column (150 × 0.50 mm × 4 μm) and eluted with 45:55 nanopure water:acetonitrile at a flow rate of 15 μL/min. The mass spectrometer was operated in negative mode with a spray voltage of 2.50 kV, gas flow rate of 10, capillary temperature of 275 °C, capillary voltage –40 V, tube lens voltage –95 V, and skimmer voltage –14 V. Data were collected over a mass range from 70.0–900.0 *m/z*. Products were identified using authentic standards by matching their retention times and exact masses.

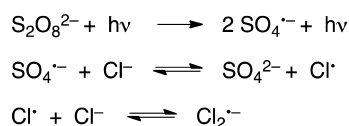
**Trapping Studies.** To address the involvement of free organic radicals in this system, photolyses were conducted using *d*<sub>8</sub>-isopropanol as a radical trap. These studies used the same conditions as the normal photolysis experiments but contained *d*<sub>8</sub>-isopropanol (1 M). Controls using isopropanol (1 M) accounted for any changes in the reaction due to the additional organic solvent. Furthermore, to test for the involvement of a heterolytic cleavage mechanism (forming a carbocation and a chloride anion) studies were conducted in the presence of high concentrations of NaCl (1 M) or NaBr (1 M). Data from this experiment are provided in the Supporting Information.

**Laser Studies.** To determine whether or not chlorine radical (Cl•) was involved in the photodegradation of triclosan, a series of transient absorption studies were performed using a previously described method.<sup>28</sup> The laser system consisted of a Solstice amplified femtosecond Ti:Sapphire laser (795 nm, 3.2 W, 80 fs; Spectra-Physics) coupled with a Topas operational parametric amplifier to modify the pump wavelength (Light Conversion). The spectrometer system consisted of an EOS transient absorption spectrometer (Ultrafast Systems). To monitor ΔAbs, the system used a sub ns supercontinuum laser pulse generated from a Nd:YAG laser coupled with a

doped optical fiber and monitored the absorbance versus time via separate reference and experimental array detectors. The ultrafast, OPA modified pump pulse was directed at a 10 mm path length quartz flow cell connected to a peristaltic pump and a 100 mL sealed reservoir.

Positive control experiments were conducted in water with  $K_2S_2O_8$  (0.02 M) as a sensitizer combined with one of NaCl, NaBr, or KSCN (0.1 M) to generate  $X^\bullet$  ( $X = Cl, Br, \text{ or } SCN$ ).  $X^\bullet$  reacts with  $X^-$  to form the radical anion  $X_2^{\bullet-}$ , which is spectroscopically observable (Scheme 1).<sup>28,29</sup>

Scheme 1



The solutions were irradiated at 285 nm (OD of solution  $\sim 0.1$ ). A solution of  $K_2S_2O_8$  without any NaCl, NaBr, or KSCN yielded no transient signal, while solutions containing these traps produced strong transients in the region from  $\sim 380$ – $650$  nm. Positive control experiments were also conducted using chlorobenzene (3 mM) in water because it is known to undergo homolytic C–Cl bond cleavage<sup>24</sup> using KSCN (0.1 M) as a trap. The solution was irradiated with a laser pulse at 275 nm. Lastly, similar experiments were performed using triclosan (110  $\mu M$ , OD 0.1 @ 316 nm) in the presence of NaCl, NaBr, or KSCN (0.1 M) in methanol. The solution was irradiated with a laser pulse at 316 nm.

**Theoretical Methods.** Initial calculations were performed using the Gaussian 09 (Rev. C.01) suite of programs.<sup>30</sup> To model the effect of the solvent on the structure and energetics of the molecules under study, the IEF-PCM method<sup>31</sup> was used with water as the implicit solvent. The long-range corrected functional, CAM-B3LYP,<sup>32</sup> was used for all calculations. A mixed basis set was used for the triclosan molecule and all triclosan fragments. For all chlorine and oxygen atoms the 6-31++G(2d,2p) basis set was used. In addition, this basis set was used for any carbon attached to a chlorine or oxygen atom. The remaining carbon and hydrogen atoms were treated with the smaller 6-31+G(d) basis set. This mixed treatment was used to give a larger and more flexible active space for the orbitals involved in bond breaking and subsequent ion or radical formation. Tests were performed on the triclosan  $S_0$  and  $S_1$  structures with 6-31++G(2d,2p) basis set applied to all atoms. The resulting geometries and vertical and adiabatic transitions were in good agreement with the reduced mixed basis set values. Therefore, the mixed basis set was used as a means of making the processor-intensive excited state calculations more tractable.

Bond energies represent the  $\Delta H$  value derived from the thermochemical parameters calculated for the optimized reactants and products at 298.15 K and 1 atm. These parameters were the result of a numeric ( $S_1$ ) or analytical ( $S_0$ ) frequency calculation at the CAM-B3LYP/mixed basis set level of theory as described above. Calculations resulting in imaginary frequencies were indicative of a nonequilibrium geometry, and the offending geometry was reoptimized until a true local minimum was found.

Additional spin-flip TD-DFT calculations were conducted using Q-Chem 4.0.<sup>33</sup> These calculations were performed in the gas phase using the B3LYP functional<sup>34</sup> and the 6-31+G\* basis

set. Background on the spin-flip methodology is available in the literature.<sup>33</sup> Briefly, the spin-flip TD-DFT method is analogous to the standard TD-DFT method except that the reference “ground state” is a triplet or quartet rather than the standard  $S_0$  ground state used for a standard TD-DFT calculation. This change in reference state allows for access to singlet biradical states, which are not properly described using traditional methods. The application of this recently developed methodology allows for the assessment of excited state homolytic cleavage processes and transient biradicals.

## RESULTS AND DISCUSSION

**Products. General.** Triclosan, long known to be more photochemically labile under basic conditions,<sup>7,9,10</sup> was photolyzed (300 nm) in basic solution (pH 10.6, 10% methanol), leading to a variety of products (Figure 1). The four primary photoproducts outlined in Figure 1 were observed: 2,8-DCDD (4%, this work),<sup>9–14</sup>  $(OH)_2PCB-13$  (10%, this work),<sup>10</sup> 5-chloro-2-(4-chlorophenoxy)phenol (0.5% this work),<sup>15</sup> and 2,4-dichlorophenol (7%, this work).<sup>15</sup> 2,8-DCDD was identified by its HPLC retention time and characteristic absorbance spectrum and quantified using an authentic standard. The remaining products were identified by their retention times and mass spectra (negative mode) and were quantified using authentic standards.

In this work, other previously assigned products were not detected in the negative mode high-resolution mass spectra. These include hydroxylated dichlorinated dibenzofuran ( $C_{12}H_5O_2Cl_2$ , 250.9667  $m/z$ ),<sup>11,14</sup> and products in which a chlorine atom is replaced by a hydroxyl group ( $C_{12}H_7O_3Cl_2$ , 268.9772  $m/z$ ),<sup>15</sup> products for which no standard was available. It should be added that the presence of these products has not been rigorously ruled out. Rather, their nondetection only signifies that scans for the exact mass of these potential products did not yield identifiable peaks in the chromatograms.

**Cyclization to 2,8-DCDD.** *Ortho*-halogen substituted phenoxyphe-nols undergo photochemically mediated cyclization reactions forming halogenated dibenzodioxins (Figure 1, I).<sup>35</sup> Dioxin formation has previously been observed with triclosan both quantitatively (3–12% conversion)<sup>9</sup> and qualitatively.<sup>10–14</sup> Analogous dioxin products have also been observed for chlorinated triclosan derivatives (0.5–2% conversion),<sup>17</sup> polychlorinated phenoxyphe-nols,<sup>18,19,21</sup> and brominated phenoxyphe-nols.<sup>22,23,36</sup>

**Rearrangement to  $(OH)_2PCB-13$ .** First suggested as a triclosan photolysis product by Wong-Wah-Chung and co-workers,<sup>10</sup> chlorinated hydroxylated biphenyls (Figure 1, II) (primary photoproduct  $C_{12}H_7O_2Cl_2$ , 252.9823  $m/z$ ) have the same molecular formula as the products of hydrodehalogenation (Figure 1, III). Authentic standards of the dichlorinated hydroxylated biphenyl (4,5'-dichloro-[1,1'-biphenyl]-2,2'-diol or  $(OH)_2PCB-13$ ) and two isomers of the monochlorinated hydroxylated biphenyl (5-chloro-[1,1'-biphenyl]-2,2'-diol and 4-chloro-[1,1'-biphenyl]-2,2'-diol or  $(OH)_2PCB-2$  and  $(OH)_2PCB-3$ ) were synthesized and were used to confirm the peak identities and/or to quantify product formation. The hydroxylated dichlorobiphenyl,  $(OH)_2PCB-13$ , accounts for 10% of the products formed from triclosan photolysis.

The mechanism of  $(OH)_2PCB-13$  formation is thought to proceed via a biradical intermediate (Figure 2, pathway C, discussed further below). The same intermediate has been proposed in the photochemical decomposition of dioxins, which yield dihydroxy-PCBs (Figure 3).<sup>37–39</sup> The proposed



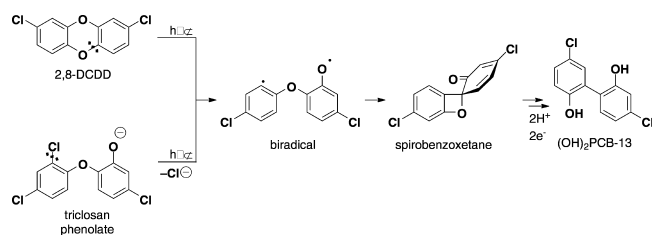


**Figure 3.** Dibenzo-*p*-dioxins and phenoxyphenols are thought to form biradical intermediates upon photochemical excitation. Prior studies<sup>37–39</sup> suggest that the biradical is a critical intermediate along the pathway to hydroxylated biphenyl formation.

mechanism of dioxin photolysis reactions involves initial cleavage of a carbon–oxygen bond forming the biradical. The biradical then rearranges to give a spirobenzoxetane and is finally reduced to give the hydroxylated biphenyl product.<sup>37–39</sup>

The previous observation of dioxin-derived dihydroxy-PCBs initially led to the hypothesis that (OH)<sub>2</sub>PCB-13 in this study was a downstream product of 2,8-DCDD, the triclosan-derived dioxin. The kinetics of product formation, however, indicated that (OH)<sub>2</sub>PCB-13 is a primary photoproduct, formed contemporaneously with 2,8-DCDD (Figure 4). Furthermore,

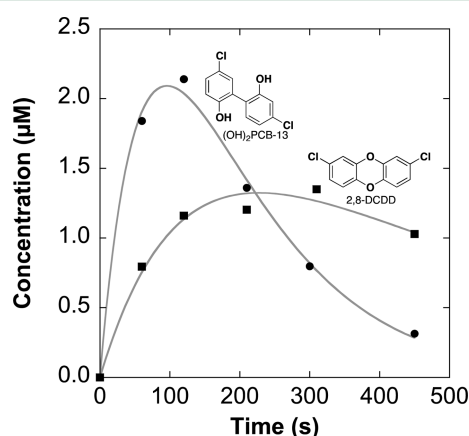


**Figure 4.** Kinetic data fitted to a growth and decay model for the formation and degradation of 2,8-DCDD (squares) and (OH)<sub>2</sub>PCB-13 (circles) from triclosan. Rate constants for (OH)<sub>2</sub>PCB-13 from the model fit were  $k_1 = 7.89 \pm 0.33 \times 10^{-3} \text{ s}^{-1}$  and  $k_2 = 1.35 \pm 0.03 \times 10^{-2} \text{ s}^{-1}$ . For 2,8-DCDD, the best fit rate constants were  $k_1 = 2.21 \pm 0.16 \times 10^{-3} \text{ s}^{-1}$  and  $k_2 = 7.68 \pm 0.52 \times 10^{-3} \text{ s}^{-1}$ .

although the triclosan-derived dioxin is photolabile, its rate of degradation ( $2.2 \times 10^{-3} \text{ s}^{-1}$ ) is slower than the rate of formation of (OH)<sub>2</sub>PCB-13 ( $1.3 \times 10^{-2} \text{ s}^{-1}$ ) (Figure 4).

(OH)<sub>2</sub>PCB-13 undergoes hydrodehalogenation, forming (5-chloro-[1,1'-biphenyl]-2,2'-diol) ((OH)<sub>2</sub>PCB-2) and/or 4-chloro-[1,1'-biphenyl]-2,2'-diol ((OH)<sub>2</sub>PCB-3), and ultimately the fully dechlorinated [1,1'-biphenyl]-2,2'-diol. The nature of the product formation for the hydrodehalogenation products is consistent with a stepwise reaction (see the Supporting Information). In the presence of *d*<sub>8</sub>-isopropanol, deuterium incorporation in (OH)<sub>2</sub>PCB-2/(OH)<sub>2</sub>PCB-3 and [1,1'-biphenyl]-2,2'-diol is consistent with a radical mechanism for hydrodehalogenation.

**Hydrodehalogenation Products: Phenoxyphenols.** Hydrodehalogenation reactions were observed in this study (Figure 5) consistent with previous reports based on mass spectroscopic analysis of triclosan photolysate.<sup>15</sup> In the current study,

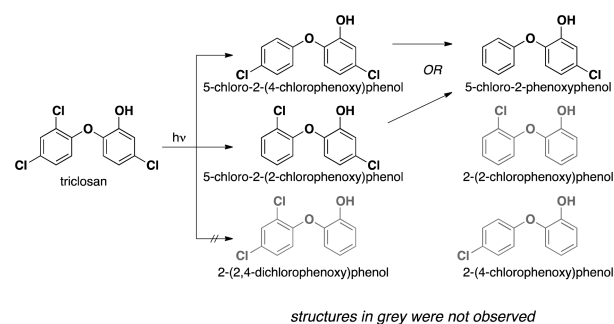


**Figure 5.** Triclosan yields phenoxyphenol photoproducts. The C–Cl bonds on the dichlorinated ring are more labile than the chlorine on the phenolate ring.

authentic standards of the hydrodehalogenation products of triclosan were independently synthesized and used to identify and quantify the observed products. Masses and retention times for the standards were compared to those observed in the triclosan photolysate using nUPLC-MS operated in negative mode. In contrast to Ferrer et al., where masses consistent with three dichlorinated congeners were observed,<sup>15</sup> two dichlorinated phenoxyphenols were assigned in this study. Of the possible dichlorinated phenoxyphenol congeners, 5-chloro-2-(4-chlorophenoxy)phenol (0.5% conversion, verified using independently synthesized authentic standard) and 5-chloro-2-(2-chlorophenoxy)phenol (tentatively assigned but not verified due to lack of authentic standard) are thought to be formed in this reaction. The third possible dichlorinated congener, 2-(2,4-dichlorophenoxy)phenol, for which an authentic standard was available through independent synthesis, was not observed, further supporting the formation of 5-chloro-2-(2-chlorophenoxy)phenol. The dichlorinated phenoxyphenols were identified by their retention times, exact mass in negative mode ( $252.9823 \text{ m/z}$ ), and their chlorine isotope patterns. As with triclosan, the dichlorinated phenoxyphenols are photolabile. A single monochlorinated phenoxyphenol isomer was observed ( $219.0213 \text{ m/z}$ ), corresponding to 5-chloro-2-phenoxyphenol. It could theoretically come from either 5-chloro-2-(4-chlorophenoxy)phenol or 5-chloro-2-(2-chlorophenoxy)phenol (Figure 5).

**Ether Cleavage Products: Chlorophenols.** The ether cleavage product, 2,4-dichlorophenol, has been observed in this study by HPLC with diode array detection and nUPLC-MS, and its identity was confirmed using an authentic standard (Figure 1, IV). In this study, 7% conversion to 2,4-dichlorophenol was observed, consistent with previous results.<sup>9</sup> The formation of 2,4-dichlorophenol suggests an ether cleavage mechanism that could also give rise to 3-chlorophenol. Although masses consistent with monochlorophenols have been observed in this study and others,<sup>14</sup> the identity of the monochlorophenol congeners were not assigned. A second possibility is that carbon–oxygen bond cleavage results in the formation of a carbene intermediate that could rearrange giving cyclopentadienylcarboxylic acids,<sup>40</sup> but no evidence for such a transformation was observed.

**Mechanisms. Excited States Involved.** Photochemical excitation of ground state ( $S_0$ ) triclosan results in the initial formation of a singlet excited state ( $S_1$ ). This excited singlet can either radiatively or nonradiatively relax back to  $S_0$  via fluorescence or internal conversion, respectively, or it can undergo intersystem crossing to the triplet state ( $T_1$ ). In principle, it can react to give products from either the  $S_1$  or  $T_1$



observed, suggesting that  $\text{Cl}^\bullet$  is not formed during the direct photolysis of triclosan in any significant amount.

Control studies were performed to observe a positive control and validate our methodology. Potassium peroxydisulfate can be used to independently generate halogen ( $\text{Cl}^\bullet$  and  $\text{Br}^\bullet$ ) and pseudohalogen ( $\text{SCN}^\bullet$ ) radicals.<sup>28</sup> These radicals go on to react with their corresponding anions to form radical anion species ( $\text{X}_2^{\bullet-}$ ), which were spectroscopically observed in this study. As an additional positive control, chlorobenzene, which is known to undergo photochemically mediated homolytic cleavage leading to  $\text{Cl}^\bullet$ ,<sup>24</sup> was photolyzed in the presence of KSCN as a chlorine radical trap. With chlorobenzene, a signal consistent with the involvement of  $\text{Cl}^\bullet$  was observed. The results of all of these experiments are in the Supporting Information.

**Reductive Cleavage Mechanism.** Reductive cleavage of C–Cl bonds has shown to be important in a variety of photochemical mechanisms.<sup>21,24</sup> In this process, excitation results in intramolecular electron transfer from the phenolate oxygen to the dichlorinated “acceptor” ring of the phenox-yphenol, effectively reducing this ring and forming a biradical anion (Figure 2, pathway C). The C–Cl bond can then cleave *irreversibly* yielding a biradical and a chloride anion. As this process is irreversible, added chloride would not influence this reaction.

Consistent with a reductive cleavage mechanism, theoretical data suggest that there is a significant change in electron density between the  $S_0$  and  $S_1$  states. Changes in electron density upon excitation from the ground state ( $S_0$ ) to the excited state ( $S_1$ ) can be visualized by evaluating the HOMO and LUMO of the  $S_0$  state. In the orbital diagrams (Figure 6) of triclosan in the  $S_0$

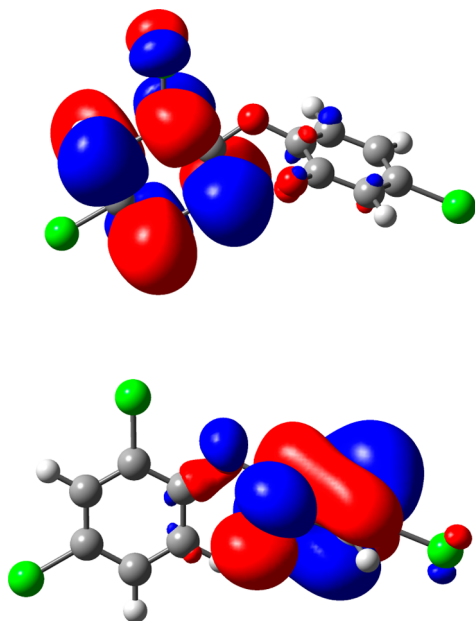


**Figure 6.** Electron density plots of the HOMO (below) and LUMO (above) orbitals of triclosan (isovalue = 0.02).

state, it is clear that upon absorption of a photon, the electron density moves from the phenolate ring in the  $S_0$  state (HOMO) to the dichloro-substituted ring in the  $S_1$  state (LUMO).

Spin-flip DFT was employed to further investigate the possibility of a biradical intermediate. This method is designed to properly describe biradical electronic states and is ideally suited to investigate the involvement of such a species in

triclosan photolysis. These calculations suggest that there is a stable, biradical excited state (333 kJ/mol relative to  $S_0$ ). In comparison to the closed-shell TD-DFT  $S_1$  energy (390 kJ/mol relative to  $S_0$ ), the biradical species is significantly lower in energy. The spin density diagram in Figure 7 illustrates the

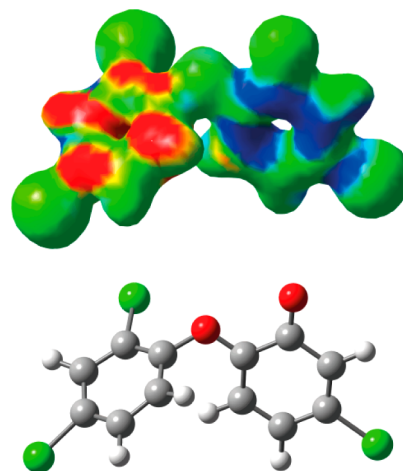


**Figure 7.** Spin density values mapped onto the electron density surface for triclosan phenolate in the first excited state, calculated using spin-flip DFT methodology (top). The electron density surface represents an isovalue of 0.03, and the (excess) spin density values range from  $-5 \times 10^{-3}$  (red, left) to  $5 \times 10^{-3}$  (red, left blue, right). Optimized biradical anion structure (bottom).

excess spin in the biradical state showing the relative separation of the two radicals (spin-up and spin-down electrons) between the rings. This picture is wholly consistent with the notion of phenolate oxidation by electron transfer to the acceptor ring.

Additionally, comparison of the potential energy surfaces obtained for the standard TD-DFT  $S_1$  (pathway B) and spin-flip TD-DFT (pathway C) suggests that the barrier to *ortho* C–Cl bond cleavage is lower for pathway C. Estimates from the potential energy curve for the biradical anion (See Supporting Information) yield a BDE of less than 10 kcal/mol for reductive *ortho* C–Cl bond cleavage (pathway C) compared to 34 kcal/mol calculated for homolytic cleavage (pathway B). The orbital diagrams and spin-flip DFT results, combined with the favorability of an intramolecular, one-step process to form the singlet biradical, support this mechanism.

It should be noted that TD-DFT is known to misrepresent the potential energy surfaces involved in homolytic cleavage at bond-lengths far from equilibrium.<sup>44</sup> For the reported  $S_1$  BDE values obtained with TD-DFT, we have avoided this issue by interrogating the systems at equilibrium, where TD-DFT is well-behaved. In this scheme, the thermodynamic energies of the bound system are compared with the sum of the energies of the products at their equilibrium  $S_1$  geometries, rather than deriving energies from potential energy scans. The spin-flip method does not suffer from this problem and allows for our semiquantitative analysis of the biradical excited state potential energy curve (see the Supporting Information).

In summary of the theoretical results, the biradical excited state is significantly lower in energy than the equilibrium  $S_1$  state, suggesting that intramolecular electron transfer in the excited state is favored. In addition, comparison of the thermodynamic BDE values from the  $S_1$  state and the potential energy curve of the spin-flip state suggest that the barrier to loss of chloride from the biradical state is comparable in energy, if



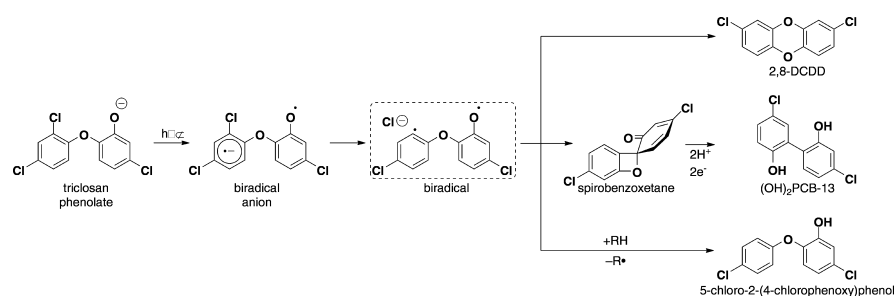


**Figure 8.** Upon light absorption, triclosan phenolate is thought to undergo intramolecular electron transfer leading to a biradical anion. Subsequent cleavage of the *ortho* C–Cl bond yields a biradical that can couple to give 2,8-DCDD, rearrange to give (OH)<sub>2</sub>-PCB-13, or abstract a hydrogen atom to give 5-chloro-2-(4-chlorophenoxy)phenol.

not less than, the barrier to loss of the chlorine atom radical from the S<sub>1</sub> state. These results, in concert with the experimental data, support the involvement of a biradical intermediate in the formation of 2,8-DCDD and (OH)<sub>2</sub>-PCB-13.

**Product Formation from Biradical.** A biradical intermediate is likely the critical intermediate in dioxin, biphenyl, and phenoxyphenol formation (Figure 8). The phenoxy and carbon-based radicals couple to form the observed dioxin. Quenching of the carbon-based radical via hydrogen atom abstraction (from the solvent) would readily give the hydrodehalogenation products. Hydrogen atom abstraction is likely to be enhanced in the presence of an organic cosolvent (methanol in this case), and this product may form less readily in pure water. The mechanism to form the dichlorinated hydroxylated biphenyl proceeds via the mechanism previously proposed for hydroxylated biphenyl formation (Figure 3).<sup>37–39</sup>

**Mechanistic Overview.** Upon photochemical irradiation, triclosan readily degrades, forming a variety of products including 2,8-DCDD, (OH)<sub>2</sub>-PCB-13, dechlorinated triclosan, and 2,4-dichlorophenol. Both the experimental and computational results indicate that the first three products are derived from a biradical intermediate formed via reductive cleavage of the *ortho*-carbon chlorine bond in triclosan. This intermediate can couple, rearrange, or abstract a hydrogen atom from the solvent yielding the observed products.

## ■ ASSOCIATED CONTENT

### Supporting Information

Data from the trapping study, formation and degradation data for the hydroxylated biphenyls, chromatograms and mass spectra for observed products, laser flash photolysis results and computational data. This material is available free of charge via the Internet at <http://pubs.acs.org>.

## ■ AUTHOR INFORMATION

### Corresponding Author

\*Phone: +41 44 632 47 55. Fax: +41 44 632 14 38. E-mail: kris.mcneill@env.ethz.ch.

### Present Address

<sup>†</sup>Department of Chemistry, Bowdoin College, 6600 College Station, Brunswick, ME 04011.

### Notes

The authors declare no competing financial interest.

## ■ ACKNOWLEDGMENTS

We gratefully acknowledge support from ETH and the U.S. National Science Foundation (CBET-0967163).

## ■ REFERENCES

- (1) Bock, M.; Lyndall, J.; Barber, T.; Fuchsman, P.; Perruchon, E.; Capdevielle, M. Probabilistic application of a fugacity model to predict triclosan fate during wastewater treatment. *Integr. Environ. Assess. Manage.* **2010**, 6 (3), 393–404.
- (2) Singer, H.; Müller, S.; Tixier, C.; Pillonel, L. Triclosan: Occurrence and fate of a widely used biocide in the aquatic environment: field measurements in wastewater treatment plants, surface waters, and lake sediments. *Environ. Sci. Technol.* **2002**, 36 (23), 4998–5004.
- (3) Kolpin, D. W.; Furlong, E. T.; Meyer, M. T.; Thurman, E. M.; Zaugg, S. D.; Barber, L. B.; Buxton, H. T. Pharmaceuticals, hormones, and other organic wastewater contaminants in US streams, 1999–2000: a national reconnaissance. *Environ. Sci. Technol.* **2002**, 36 (6), 1202–1211.
- (4) Cantwell, M. G.; Wilson, B. A.; Zhu, J.; Wallace, G. T.; King, J. W.; Olsen, C. R.; Burgess, R. M.; Smith, J. P. Temporal trends of triclosan contamination in dated sediment cores from four urbanized estuaries: evidence of preservation and accumulation. *Chemosphere* **2010**, 78 (4), 347–352.
- (5) Miller, T. R.; Heidler, J.; Chillrud, S. N.; Delaquil, A.; Ritchie, J. C.; Mihalic, J. N.; Bopp, R.; Halden, R. U. Fate of triclosan and evidence for reductive dechlorination of triclosan in estuarine sediments. *Environ. Sci. Technol.* **2008**, 42 (12), 4570–4576.
- (6) Lindstrom, A.; Buerge, I. J.; Poiger, T.; Bergqvist, P. A.; Müller, M. D.; Buser, H. R. Occurrence and environmental behavior of the bactericide triclosan and its methyl derivative in surface waters and in wastewater. *Environ. Sci. Technol.* **2002**, 36 (11), 2322–2329.
- (7) Tixier, C.; Singer, H.; Canonica, S.; Müller, S. R. Photo-transformation of triclosan in surface waters: a relevant elimination process for this widely used biocide - laboratory studies, field measurements, and modeling. *Environ. Sci. Technol.* **2002**, 36 (16), 3482–3489.
- (8) Bedoux, G.; Roig, B.; Thomas, O.; Dupont, V.; Le Bot, B. Occurrence and toxicity of antimicrobial triclosan and by-products in the environment. *Environ. Sci. Pollut. Res.* **2012**, 19 (4), 1044–1065.
- (9) Latch, D. E.; Packer, J. L.; Stender, B. L.; VanOverbeke, J.; Arnold, W. A.; McNeill, K. Aqueous photochemistry of triclosan: formation of 2,4-dichlorophenol, 2,8-dichlorodibenzo-p-dioxin, and oligomerization products. *Environ. Toxicol. Chem.* **2005**, 24 (3), 517–525.
- (10) Wong-Wah-Chung, P.; Rafqah, S.; Voyard, G.; Sarakha, M. Photochemical behaviour of triclosan in aqueous solutions: kinetic and analytical studies. *J. Photochem. Photobiol., A* **2007**, 191 (2–3), 201–208.
- (11) Kanetoshi, A.; Ogawa, H.; Katsura, E.; Kaneshima, H. Chlorination of Irgasan DP300 and formation of dioxins from its chlorinated derivatives. *J. Chromatogr.* **1987**, 139–153.
- (12) Latch, D. E.; Packer, J. L.; Arnold, W. A.; McNeill, K. Photochemical conversion of triclosan to 2,8-dichlorodibenzo-p-dioxin in aqueous solution. *J. Photochem. Photobiol., A* **2003**, 158 (1), 63–66.
- (13) Mezcu, M.; Gomez, M. J.; Ferrer, I.; Agüera, A.; Hernando, M. D.; Fernandez-Alba, A. R. Evidence of 2,7/2,8-dibenzodichloro-p-



dioxin as a photodegradation product of triclosan in water and wastewater samples. *Anal. Chim. Acta* **2004**, 524 (1–2), 241–247.

(14) Sanchez-Prado, L.; Llompart, M.; Lores, M.; Fernandez-Alvarez, M.; Garcia-Jares, C.; Cela, R. Further research on the photo-SPME of triclosan. *Anal. Bioanal. Chem.* **2006**, 384 (7–8), 1548–1557.

(15) Ferrer, I.; Mezcu, M.; Gómez, M. J.; Thurman, E. M.; Agüera, A.; Hernando, M. D.; Fernández-Alba, A. R. Liquid chromatography/time-of-flight mass spectrometric analyses for the elucidation of the photodegradation products of triclosan in wastewater samples. *Rapid Commun. Mass Spectrom.* **2004**, 18 (4), 443–450.

(16) Chen, Z.; Cao, G.; Song, Q. Photo-polymerization of triclosan in aqueous solution induced by ultraviolet radiation. *Environ. Chem. Lett.* **2008**, 8 (1), 33–37.

(17) Buth, J. M.; Grandbois, M.; Vikesland, P. J.; McNeill, K.; Arnold, W. A. Aquatic photochemistry of chlorinated triclosan derivatives: potential source of polychlorodibenzo-p-dioxins. *Environ. Toxicol. Chem.* **2009**, 28 (12), 2555–2563.

(18) Freeman, P. K.; Srinivasa, R. Photochemistry of polychlorinated phenoxyphenols: photochemistry of 3,4,5,6-tetrachloro-2-(pentachlorophenoxy)phenol. *J. Agric. Food Chem.* **1983**, 31, 775–780.

(19) Freeman, P. K.; Srinivasa, R. Photochemistry of polychlorinated phenoxyphenols. 3. Solvent effects on the photochemical transformation of 3,4,5,6-tetrachloro-2-(pentachlorophenoxy)phenol. *J. Agric. Food Chem.* **1984**, 32 (6), 1313–1316.

(20) Freeman, P. K.; Jonas, V. Photochemistry of polychlorinated phenoxyphenols. 2. Phototransformations of *m*-(pentachlorophenoxy)-2,4,5,6-tetrachlorophenol. *J. Agric. Food Chem.* **1984**, 32 (6), 1307–1313.

(21) Freeman, P. K.; Srinivasa, R. Photochemistry of polyhaloarenes. 4. Phototransformations of perchloro-*o*-phenoxyphenol in basic media. *J. Org. Chem.* **1986**, 51 (21), 3939–3942.

(22) Erickson, P. R.; Grandbois, M.; Arnold, W. A.; McNeill, K. Photochemical formation of brominated dioxins and other products of concern from hydroxylated polybrominated diphenyl ethers (OH-PBDEs). *Environ. Sci. Technol.* **2012**, 46 (15), 8174–8180.

(23) Steen, P. O.; Grandbois, M.; McNeill, K.; Arnold, W. A. Photochemical formation of halogenated dioxins from hydroxylated polybrominated diphenyl ethers (OH-PBDEs) and chlorinated derivatives (OH-PBCDEs). *Environ. Sci. Technol.* **2009**, 43 (12), 4405–4411.

(24) Schutt, L.; Bunce, N. J. Photodehalogenation of aryl halides. In *CRC Handbook of Organic Photochemistry and Photobiology*, 2nd ed.; Horspool, W., Lenci, F., Eds.; CRC Press LLC: 2003; pp 38/1–38/18.

(25) Liu, C.; Ni, Q. J.; Bao, F. Y.; Qiu, J. S. A simple and efficient protocol for a palladium-catalyzed ligand-free Suzuki reaction at room temperature in aqueous DMF. *Green Chem.* **2011**, 13 (5), 1260–1266.

(26) Marcoux, J.-F.; Doye, S.; Buchwald, S. L. A general copper-catalyzed synthesis of diaryl ethers. *J. Am. Chem. Soc.* **1997**, 119 (43), 10539–10540.

(27) Yeager, G. W.; Schissel, D. N. An unpoled synthon approach to the synthesis of 2-aryloxyphenols. *Synthesis* **1995**, 1, 28–30.

(28) Nagarajan, V.; Fessenden, R. W. Flash photolysis of transient radicals. 1. X<sub>2</sub>- with X = Cl, Br, I, and SCN. *J. Phys. Chem.* **1985**, 89 (11), 2330–2335.

(29) Yu, X. Y.; Bao, Z. C.; Barker, J. R. Free radical reactions involving Cl-center dot, Cl-2(-center dot), and SO<sub>4</sub>-center dot in the 248 nm photolysis of aqueous solutions containing S<sub>2</sub>O<sub>8</sub><sup>2-</sup> and Cl<sup>-</sup>. *J. Phys. Chem. A* **2004**, 108 (2), 295–308.

(30) Frisch, M. J.; Trucks, G. W.; Schlegel, H. B.; Scuseria, G. E.; Robb, M. A.; Cheeseman, J. R.; Scalmani, G.; Barone, V.; Mennucci, B.; Petersson, G. A.; Nakatsuji, H.; Caricato, M.; Li, X.; Hratchian, H. P.; Izmaylov, A. F.; Bloino, J.; Zheng, G.; Sonnenberg, J. L.; Hada, M.; Ehara, M.; Toyota, K.; Fukuda, R.; Hasegawa, J.; Ishida, M.; Nakajima, T.; Honda, Y.; Kitao, O.; Nakai, H.; Vreven, T.; Montgomery, J. A., Jr.; Peralta, J. E.; Ogliaro, F.; Bearpark, M.; Heyd, J. J.; Brothers, E.; Kudin, K. N.; Staroverov, V. N.; Kobayashi, R.; Normand, J.; Raghavachari, K.; Rendell, A.; Burant, J. C.; Iyengar, S. S.; Tomasi, J.; Cossi, M.; Rega, N.; Millam, J. M.; Klene, M.; Knox, J. E.; Cross, J. B.; Bakken, V.; Adamo, C.; Jaramillo, J.; Gomperts, R.; Stratmann, R. E.; Yazyev, O.;

Austin, A. J.; Cammi, R.; Pomelli, C.; Ochterski, J. W.; Martin, R. L.; Morokuma, K.; Zakrzewski, V. G.; Voth, G. A.; Salvador, P.; Dannenberg, J. J.; Dapprich, S.; Daniels, A. D.; Farkas, Ö.; Foresman, J. B.; Ortiz, J. V.; Cioslowski, J.; Fox, D. J. *Gaussian 09 Revision C.01*; Gaussian Inc.: Wallingford, CT, 2009.

(31) Tomasi, J.; Mennucci, B.; Cammi, R. Quantum mechanical continuum solvation models. *Chem. Rev.* **2005**, 105 (8), 2999–3094.

(32) Yanai, T.; Tew, D. P.; Handy, N. C. A new hybrid exchange–correlation functional using the Coulomb-attenuating method (CAM-B3LYP). *Chem. Phys. Lett.* **2004**, 393 (1–3), 51–57.

(33) Shao, Y. H.; Head-Gordon, M.; Krylov, A. I. The spin-flip approach within time-dependent density functional theory: Theory and applications to diradicals. *J. Chem. Phys.* **2003**, 118 (11), 4807–4818.

(34) Becke, A. D. Density-functional thermochemistry. III. The role of exact exchange. *J. Chem. Phys.* **1993**, 98 (7), 5648–5652.

(35) Nilsson, C.; Andersson, K.; Rappe, C.; Westermark, S. Chromatographic evidence for the formation of chlorodioxins from chloro-2-phenoxyphenols. *J. Chromatogr.* **1974**, 96 (1), 137–147.

(36) Arnoldsson, K.; Andersson, P. L.; Haglund, P. Photochemical formation of polybrominated dibenzo-p-dioxins from environmentally abundant hydroxylated polybrominated diphenyl ethers. *Environ. Sci. Technol.* **2012**, 46 (14), 7567–7574.

(37) Guan, B.; Wan, P. Photochemistry of dibenzo-1,4-dioxins: intramolecular rearrangement-reduction through observable 2,2'-biphenylquinones. *J. Photochem. Photobiol., A* **1994**, 80 (1–3), 199–210.

(38) Rayne, S.; Sasaki, R.; Wan, P. Photochemical rearrangement of dibenzo[1,4]dioxins proceeds through reactive spirocyclohexadienone and biphenylquinone intermediates. *Photochem. Photobiol. Sci.* **2005**, 4 (11), 876–886.

(39) Rayne, S.; Wan, P.; Ikononou, M. G.; Konstantinov, A. D. Photochemical mass balance of 2,3,7,8-TeCDD in aqueous solution under UV light shows formation of chlorinated dihydroxyphenyls, phenoxyphenols, and dechlorination products. *Environ. Sci. Technol.* **2002**, 36 (9), 1995–2002.

(40) Boule, P.; Guyon, C.; Lemaire, J. Photochemistry and environment. 4. Photochemical behavior of monochlorophenols in dilute aqueous solution. *Chemosphere* **1982**, 11 (12), 1179–1188.

(41) Yang, N.-C.; McClure, D. S.; Murov, S.; Houser, J. J.; Dusenbery, R. Photoreduction of acetophenone and substituted acetophenones. *J. Am. Chem. Soc.* **1967**, 89 (21), 5466–5468.

(42) Montalti, M.; Murov, S. L. *Handbook of photochemistry*; CRC: 2006; p 650.

(43) Gray, P.; Herod, A. A. Methyl radical reactions with isopropanol and methanol their ethers and their deuterated derivatives. *Trans. Faraday Soc.* **1968**, 64, 2723–2734.

(44) Giesbertz, K. J. H.; Baerends, E. J. Failure of time-dependent density functional theory for excited state surfaces in case of homolytic bond dissociation. *Chem. Phys. Lett.* **2008**, 461 (4–6), 338–342.